Dynamic aeroelastic tailoring of a strut braced wing including fatigue loads

Rajpal, Darwin; de Breuker, Roeland

Publication date
2019

Document Version
Final published version

Published in
18th International Forum on Aeroelasticity and Structural Dynamics June 10-13, 2019

Citation (APA)
Rajpal, D., & de Breuker, R. (2019). Dynamic aeroelastic tailoring of a strut braced wing including fatigue loads. In *18th International Forum on Aeroelasticity and Structural Dynamics June 10-13, 2019: Final paper/presentation agenda* Article IFASD 2019-035

International Forum on Aeroelasticity and Structural Dynamics
IFASD 2019
9-13 June 2019, Savannah, Georgia, USA

DYNAMIC AEROELASTIC TAILORING OF A STRUT BRACED WING INCLUDING FATIGUE LOADS

Darwin Rajpal[1] **and Roeland De Breuker**[1]

[1] Faculty of Aerospace Engineering
Delft University of Technology
Kluywerg 1, 2629 HS, Delft, The Netherlands
d.rajpal@tudelft.nl

Keywords: Strut Braced Wing, Gust loads, Fatigue Loads, Aeroelasticity, Structural Optimization.

Abstract: High aspect ratio strut braced aircraft can significantly reduce the induced drag. The inherent anisotropic behaviour of the composite material along with their weight saving potential can improve the performance of the aircraft during the flight. Thus, a composite strut braced aircraft is one of the promising candidates to achieve the targets set by the European Commission in Flightpath 2050 report. In their previous works, authors have developed methodologies to include gust loads using a reduced order model and account for fatigue loads through an analytical model. In this paper, previously developed methodologies are used, to carry out a stiffness and thickness optimization of a composite strut braced wing which includes critical gust loads as well as fatigue loads. The results show that a composite strut braced wing is sized by both dynamic as well as static load cases. Additionally, by accounting for fatigue through analytical model instead of a knockdown factor, a lighter wing can be obtained.

1. INTRODUCTION

In an attempt to reduce the adverse effect of commercial air travel on the environment, European Commission in the Flightpath 2050 report [1], set the goal to achieve a 75% reduction in CO_2 emissions per passenger kilometer, 90% reduction in NOx and 60% reduction in perceived noise by 2050 as compared to the aircraft in the year 2000. These objectives seem to be too ambitious for conventional designs as it is becoming increasingly difficult to extract more performance out of the well-known wing and tube configuration. Advanced technologies, along with novel design, seem to have the potential to address the required leap in performance. One of the possible technologies to increase the efficiency of the aircraft is the application of composite materials. In addition to being beneficial in weight savings due to high specific strength, composite materials are also advantageous because of their inherent anisotropic behaviour. The directional stiffness properties of the composite material can be tailored to achieve beneficial aeroelastic deformations and hence improved performance during the flight, thus providing higher efficiency with a minimum weight penalty.

With respect to unconventional designs, a Strut Braced Wing (SBW) is one of the potential candidates to meet future societal and environmental challenges. Bending moment relief of the main wing provided by the strut leads to an increase in aspect ratio without the significant weight penalty that is observed in a cantilever wing. A high aspect ratio wing can significantly

reduce the induced drag, which is one of the significant contributors of the drag experienced by the aircraft during its entire mission. It accounts for about 30-40% of the airplane drag during the cruise and about 80-90% of the aircraft drag at low speeds [2]. A reduction in the spanwise bending moment also leads to a reduction in thickness to chord ratio and chord length. A decrease in airfoil thickness reduces the wave drag resulting in a lower sweep angle. A shorter chord length results in lower Reynolds number which, along with thinner wings, leads to more laminar flow [3, 4]. A reduction in drag combined with saving in structural weight makes a composite strut braced aircraft as one of the promising candidates to achieve the required improvement in the efficiency.

Significant work on SBW has been carried out by Virginia Tech Multidisciplinary Aircraft Design Group [5–9]. The Subsonic Ultra Green Aircraft Research (SUGAR) team led by The Boeing Company has also investigated a SBW concept as a part of NASA N+3 concept studies [10]. Results from these studies show the potential of a SBW and a Truss Braced Wing (TBW) designs to achieve a reduced take-off gross weight (TOGW) and fuel consumption compared to cantilever configurations. However, in these studies, for structural optimization, quasi-steady load definitions were used to include the influence of dynamic gust by defining, an additional scaling factor for the loads from the wingstrut joint to the wing tip [11]. A high aspect ratio composite strut braced wing has increased flexibility, which could make it more susceptible to gust loads. Thus a dynamic load analysis needs to be performed to calculate the effect of gust loads on the strut braced wing.

Taking into account gust loads during the initial phase of the design process is quite challenging as one has to scan approximately 10 million load cases to identify the worst case gust load [12]. Additionally, after every iteration, there is an update in the design which changes the aeroelastic properties of the wing leading to a change in critical gust load. Thus a rescan of all the load cases is required at every new iteration in the design. The authors [13] in their previous work have developed a methodology to include efficiently critical gust loads in the aeroelastic optimization of composite wings using the TU Delft in-house preliminary aeroelastic design tool PROTEUS. In the current paper, a similar methodology will be applied to perform dynamic aeroelastic optimization of a composite strut braced wing.

As composite wing designs become more optimized for improved aeroelastic behaviour, the difference between the magnitude of typical fatigue loads and ultimate static strength of design becomes smaller. As a result, fatigue loading, which, historically, was not a design driver for a composite structure, now becomes more important and may impact the design. The authors, in their previous work [14] developed an analytical model to predict the fatigue life of composite structures. This model was integrated into PROTEUS to perform stiffness and thickness optimization of a composite wing taking into account fatigue as one of the constraints.

With an aim to combine the methodologies developed for gust and fatigue loads and apply it to a novel configuration, in the present work, a dynamic aeroelastic optimization including the effects of critical gust and fatigue loads will be performed on a composite strut braced wing.

2. AEROELASTIC FRAMEWORK

For the sake of completeness, in this section, a brief overview of the methodology to include dynamic loads [13] and fatigue loads [14] in the aeroelastic tailoring of composite wings that was developed in the author's previous works is described.

PROTEUS [15], an in-house aeroelastic tool, developed at the Delft University of Technology, is used to carry out the optimization of a composite strut braced wing. Figure 1 depicts the schematic representation of the framework of the PROTEUS. In the first step, the wing is discretized into multiple spanwise panels. One or more laminates define each panel in the chord wise direction. In the next step, the discretized geometry is fed into a cross sectional modeller which is especially developed to deal with anisotropic shell cross-sections. The cross sectional modeller uses the cross-sectional geometry and the laminate properties to generate the Timoshenko stiffness matrices. The geometrically nonlinear Timoshenko beam model is then coupled with an unsteady vortex lattice aerodynamic model to perform geometrically non linear aeroelastic analysis for multiple load cases. Around the obtained nonlinear static equilibrium solution, a linear dynamic aeroelastic analysis is carried out. The strains in the three-dimensional wing and strut structure are retrieved using the cross sectional modeller which are then used to calculate the strength and buckling properties of the wing and the strut.

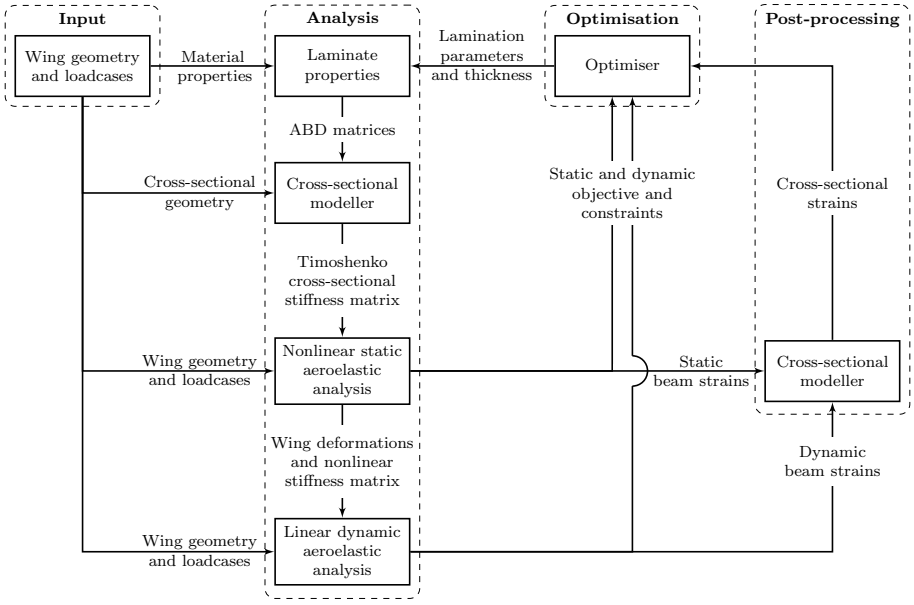

Figure 1: Framework of PROTEUS [15].

2.1. Dynamic Loads

As was mentioned before, the entire flight envelope needs to be scanned, to identify the worst case gust loads. As a result, PROTEUS needs to perform dynamic aeroelastic analysis over a large number of load cases. This can become computationally expensive. To improve the efficiency of identifying the critical dynamic loads, model order reduction (MOR) techniques are applied to reduce the aeroelastic system in PROTEUS. To formulate the reduced order aeroelastic model (ROAM), the aeroelastic system is reduced by applying the MOR method to the time-domain state-space unsteady vortex lattice model [16] and coupling it to the structural solver. In PROTEUS the aerodynamic model is based on the potential flow over a three-dimensional wing described by the Laplace equation, and rewritten into the form of a state-space system:

$$\dot{\mathbf{x}}_a = \mathbf{A}_a \mathbf{x}_a + \mathbf{B}_a \mathbf{u}, \tag{1}$$

$$\mathbf{y}_a = \mathbf{C}_a \mathbf{x}_a + \mathbf{D}_a \mathbf{u}, \tag{2}$$

where $\mathbf{A}_a$ is the state matrix, $\mathbf{B}_a$ is the input matrix, $\mathbf{u}$ is the input vector containing the time derivative of the angle of attack per aerodynamic panel of the wing, and $\mathbf{x}_a$ is the state vector containing the vortex strengths in the wake and angles of attack. The dot over the $\mathbf{x}_a$ indicates the time derivative. Additionally, $\mathbf{y}_a$ is the output vector containing the forces and moments acting on the wing per spanwise section, $\mathbf{C}_a$ is the output matrix and $\mathbf{D}_a$ is the feed through matrix. A more elaborate description of the aerodynamic modelling can be found in the work of Werter et al. [16]. To develop a reduced aerodynamic system, the original states of the linear time-invariant (LTI) state-space system is projected onto a reduced basis:

$$\mathbf{x}_a = \mathbf{V}_r \mathbf{c}, \tag{3}$$

where $\mathbf{c}$ is a vector with the r reduced states and $\mathbf{V}_r$ is the reduced basis onto which the original states are projected. Inserting this equation into equations (1) and (2), results in

$$\begin{aligned} \dot{\mathbf{c}} &= \mathbf{V}_r^{-1}\mathbf{A}_a\mathbf{V}_r\mathbf{c} + \mathbf{V}_r^{-1}\mathbf{B}_a\mathbf{u} = \mathbf{A}_r\mathbf{c} + \mathbf{B}_r\mathbf{u} \\ \mathbf{y}_a &= \mathbf{C}_a\mathbf{V}_r\mathbf{c} + \mathbf{D}_a\mathbf{u} = \mathbf{C}_r\mathbf{c} + \mathbf{D}_a\mathbf{u} \end{aligned} \tag{4}$$

The number of states in the vector $\mathbf{x}_a$ is typically in the order of $10^3 \sim 10^4$. By applying MOR methods, the dimension of the state vector $\mathbf{x}_a$ can be reduced, leading to increased computational efficiency. In the current study, balanced proper orthogonal decomposition (BPOD) method was chosen to compute the reduced basis for the aerodynamic system.

For determination of critical loads, the aeroelastic system must be solved over a large number of flight points to calculate the various responses of the aircraft over the entire flight envelope. However, the aerodynamic system depends on parameters such as altitude, Mach number and velocity. In the current methodology, the state space system described by Equation 4 is rewritten such that the reduced order aerodynamic system is independent of Mach number and velocity. With this approach, the reduced order aerodynamic system can be used along the entire flight envelope without the need of performing a new reduction at each flight point. This reduced order aerodynamic system replaces the full order unsteady aerodynamic model in the PROTEUS framework to formulate a ROAM.

Using the ROAM, an optimization framework, depicted in Figure 2, is formulated, which can identify the critical gust load at every iteration and analyze them in a computationally efficient manner. The process starts with the identifying for the initial design, the worst dynamic and static loads using the ROAM. Next, PROTEUS analyzes the initial design with respect to the identified critical loads and calculates the analytical sensitivities which are then fed to the optimizer. Based on the sensitivities, the optimizer calculates the new design variables and feeds it to both ROAM as well as PROTEUS. ROAM identifies the critical loads for the new design and feeds it back to PROTEUS. The process continues until an optimum has been reached. Since the analytical sensitivities of the objective function and constraints, including the sensitivities of the critical dynamic loads, are available, the gradient based optimizer Globally Convergent Method of Moving Asymptotes (GCMMA) developed by Svanberg [17] is used.

2.2. Fatigue Loads

To model fatigue of a composite wing, an analytical model based on Kassapoglou [18–20] method which uses a residual strength wear out model has been formulated. The fatigue model works with lamination parameters which describe the in-plane and out-of-plane behaviour of

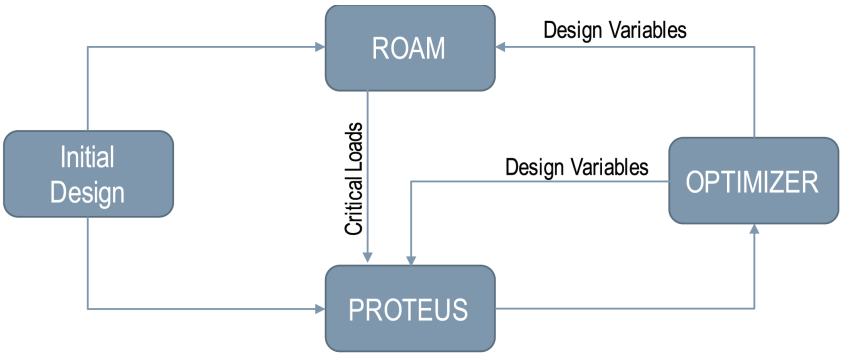

Figure 2: Schematic representation of the optimization framework.

the composite laminates and were first introduced by Tsai and Pagano [21]. Figure 3 depicts the flowchart of the fatigue model to determine failure for a composite in the lamination parameter domain. The relevant steps involved in assessing the fatigue life are summarized below.

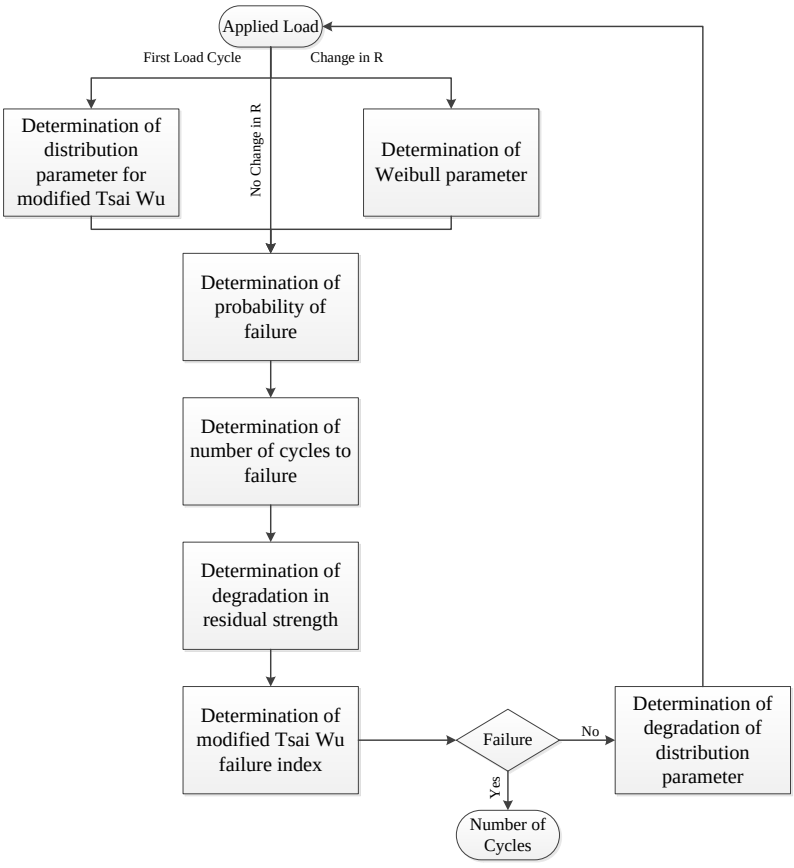

Figure 3: Algorithm for the fatigue model.

1. For the given loads, in the first load cycle, the statistical distribution of the modified Tsai Wu criterion is calculated. The Tsai Wu failure criterion in its original form explicitly depends on the ply angles and the stacking sequence. To adapt it for the lamination parameters, Khani et al. [22] formulated a failure envelope based on the conservative approximation of the Tsai-Wu failure criterion that does not explicitly depend on the ply angle. In the current fatigue model, for the failure criterion, this modified Tsai-Wu failure

envelope is implemented.

2. The probability of failure p is calculated by comparing the modified Tsai-Wu criterion of the entire laminate to the failure index, which at the start is equal to 1. The value of p also depends on the type of statistical distribution and stress ratio R.
3. Once the probability of failure is determined, the number of cycles to failure [18], N, if the failure mode does not change and p is constant, is determined by

$$N = -\frac{1}{\ln(1-p)} \tag{5}$$

4. Residual strength of the ply σ_r after n cycles of the applied strain is determined through a degradation model given by

$$\sigma_r = \sigma_{sf}(1 - (1 - \frac{\epsilon_i}{\epsilon_{sf}})\frac{n}{N-1} \tag{6}$$

where ϵ_i represents the principal strain of the laminate based on the applied stress, ϵ_{sf} represents the principal strain at which the laminate will fail and σ_{sf} is the static failure strength.

5. If the modified Tsai Wu failure criterion calculated using the degraded residual strength is higher than the failure index, the laminate fails. Otherwise, distribution parameters of the modified Tsai-Wu criterion are degraded by R_{tw} and the process continues until the maximum number of cycles has been reached, or the laminate has failed. R_{tw} is expressed as

$$R_{tw} = \frac{f}{f_r} \tag{7}$$

where f is the value of the modified Tsai-Wu criterion before the residual strength degradation and f_r is the value of the modified Tsai-Wu criterion after the residual strength degradation.

The formulated analytical fatigue model is integrated into PROTEUS. To analyze the wing for fatigue, a shortened version of the TWIST spectrum (Mini-TWIST) [23] is used as the load spectrum. A fatigue factor F is calculated for every laminate by subjecting it to Mini-TWIST spectrum for 10 times. F is defined as

$$F = r\frac{N_t}{N_f} \tag{8}$$

where r is the modified Tsai-Wu failure criterion at the time of failure, N_t represents the total cycles the structure has to withstand and N_f represents the total cycles to failure. If the laminate does not fail after the 40,000 flights, r is then the maximum modified Tsai-Wu failure criterion calculated in the spectrum.

3. OPTIMIZATION

3.1. Baseline Design

For the current study, the baseline design of the strut braced wing is based on the study performed in the Multidisciplinary Design Optimization (MDO) analysis of a composite strut

braced wing [24, 25] in the AGILE [26] which is EU funded H2020 research project. The main characteristics of the design are summarized in Table 1. Figure 4 depicts the wing planform. The wing consists of 25 ribs with a rib spacing of 0.55 m that are taken into account as concentrated masses. Additionally, fuel, engine and landing gear are also accounted for as concentrated masses. The wing strut, as well as the strut fuselage connection, is considered to be clamped.

Table 1: Characteristics of the SBW wing.

Parameter	Value	Unit
Wing Span	40.7	m
Wing sweep	16	deg
Wing aspect ratio	17.7	(-)
Wing area	93.7	m^2
Wing Root Chord	3.3	m
Strut Span	9.8	m
Strut aspect ratio	9.7	(-)
Strut Root chord	1	m
Wing Strut location	10.2	m
Cruise Mach	0.78	(-)
Design Range	3500	km
Design Payload	9180	kg
Maximum takeoff weight	39,000	kg

3.2. Optimization Setup

In the current study, two optimizations are performed: one, a dynamic aeroelastic optimization without fatigue as a constraint, and two, a dynamic aeroelastic optimization with fatigue as a constraint. In the first optimization, a knockdown factor of 0.312 is applied to the strength allowables to account for fatigue, damage and material scatter and environment. In the second optimization, a knockdown factor of 0.52 is applied to account for damage and environment. The AS4/8552 carbon/epoxy composite is used as the reference material. Table 2 shows the material properties.

The optimization setup for the current study is shown in Table 3. The objective is the minimization of the structural weight of the wing and the strut. The wing is divided into 7 spanwise sections and strut is represented by a single section. In each section, the top skin, the bottom skin and spars consist of one laminate each in the chordwise direction resulting in 32 unique

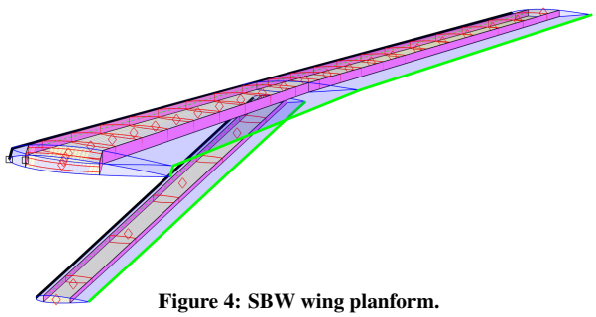

Figure 4: SBW wing planform.

laminates. The laminates are described by lamination parameters instead of stacking sequence and ply angles. The advantage of lamination parameter is that the number of design variables is reduced since a fixed number of lamination parameters describe the entire laminate irrespective of the number of plies. Additionally, lamination parameters are continuous, a gradient-based optimizer can be used, making the optimization process more efficient. Each laminate is represented by eight lamination parameters and one thickness variable resulting in a total number of 288 design variables. The laminate distribution of the top skin of the wing is shown in Figure 5. The Figure also depicts the stiffness for each laminate, where the wing stiffness distribution is represented by the polar plot of thickness normalized modulus of elasticity $\hat{\mathbf{E}}_{11}(\theta)$ which is given by

$$\hat{\mathbf{E}}_{11}(\theta) = \frac{1}{\hat{\mathbf{A}}_{11}^{-1}(\theta)} \tag{9}$$

where $\hat{\mathbf{A}}$ is the thickness normalized membrane stiffness matrix and θ ranges from 0 to 360 degrees.

Table 2: Material Properties.

Property	Value
E_{11}	128 GPa
E_{22}	9.3 GPa
G_{12}	4.8 GPa
ν_{12}	0.3 GPa
ρ	1600 $\mathrm{kg/m^3}$
X_t	1996 MPa
X_c	1398 MPa
Y_t	64 MPa
Y_c	268 MPa
S	92 MPa

Table 3: Optimization Setup.

Type	Parameter	# responses
Objective	Minimize Wing Mass	1
Design Variables	Lamination Parameter	288
	Laminate Thickness	
Constraints	Laminate Feasibility	160
	Static Strength	832/load case
	Local Buckling	2048/load case
	Strut Global Buckling	5/load case
	Fatigue	662
	Aeroelastic Stability	10/load case
	Local Angle of Attack	26/load case

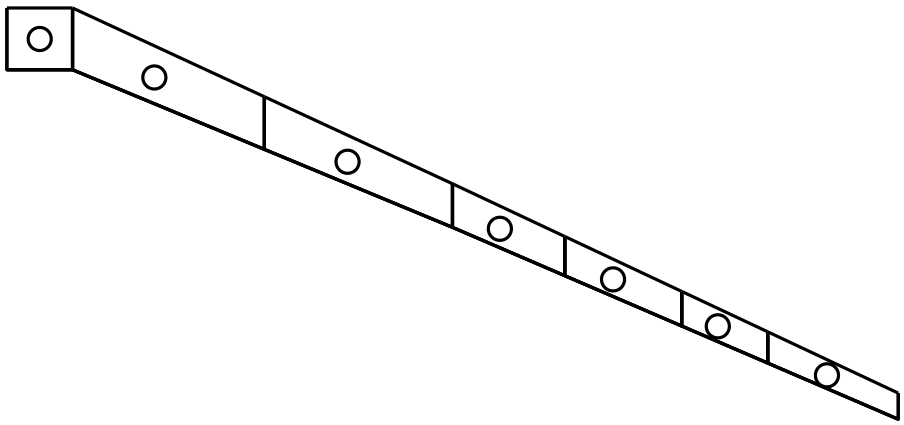

Figure 5: Laminate Distribution of the top skin of SBW.

Lamination parameters are constrained such that they represent actual ply distributions by applying lamination feasibility equations formulated by Hammer et al. [27], Raju et al. [28] and Wu et al. [29]. Tsai-Wu criterion formulated for lamination parameter domain by Khani et al. [22] is used to assess the static strength of the laminate. The stability of the panel in buckling is based on an idealized buckling model formulated by Dillinger et al. [30]. To make sure the strut does not buckl globally, the out of plane displacement of the strut beam element is con-

strained to a maximum of 0.5 m. Aeroelastic stability of the wing is ensured by constraining the real part of the eigenvalues of the state matrix to be less than zero within the flutter flight envelope. The local angle of attack is constrained to a maximum of 12 degrees and a minimum of -12 degrees.

The static load cases used in the current study are depicted in Table 4. These load cases, represent the 1g cruise condition, flutter boundary, 2.5g symmetric pull up manoeuvre and -1g symmetric push down manoeuvre.

Concerning dynamic load cases, 67 flight points representing the entire flight envelope are considered. For each flight point, 40 gust gradient both positive as well as negative, ranging from 9 m to 107 m are analyzed. For each flight point and gust gradient, two mass cases; full fuel and zero fuel are considered. Thus, in total, 5,360 load cases will be scanned to determine the critical loads. Figure 6 displays the flight envelope with their respective flight point ID.

Table 4: List of Static Loadcases.

Loadcase ID	$\mathbf{V_{eq}}$ (m/s)	**Altitude** (m)	**Load Factor**
1	125.4	11000	1
2	144	11000	1
3	125.4	11000	2.5
4	125.4	11000	-1

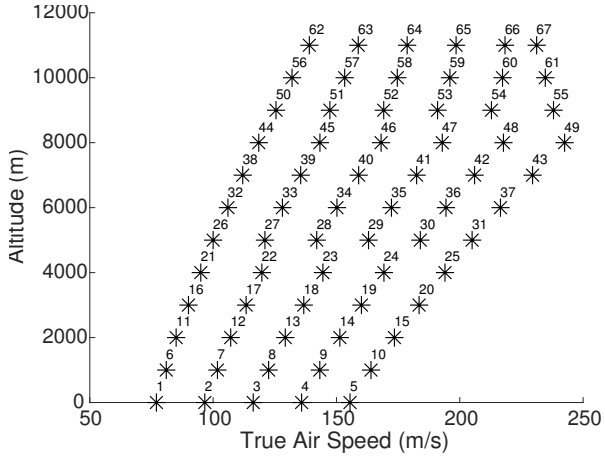

Figure 6: Flight Envelope.

3.3. Results

For both the studies, one with and one without the analytical fatigue model, Figure 7 and 8 depict the critical constraints for the strut and the wing, respectively. For the case of simplicity, from here on, the optimization without the fatigue model will be referred to as the first study and the optimization with the fatigue model will be referred to as the second study. For both the studies, the main wing is mainly dominated by strain constraints, whereas the buckling is critical in only a few panels. The strut in both the studies is critical in local as well as global buckling and also in strain. For the second study, even though the fatigue factor is not at its maximum, few panels in the middle part and inboard part of the main wing are at 80 % of the

maximum allowable fatigue limit.

Figure 9 and 10 shows the stiffness and the thickness distribution of the optimization studies for the wing and the strut respectively. As the strut is critical in both buckling as well as in strain, there is a pronounced effect on both the in plane stiffness and the out of plane stiffness. With respect to the main wing, as strain constraints mainly dominate the wing, the in plane stiffness is oriented in the forward direction at the root and the outboard part to introduce wash-out twist upon wing bending which alleviates the load. In the middle part, the in plane stiffness is oriented along the wing axis to maximize the load carrying capabilities. In the case of the second study, fatigue plays a role in orienting the in plane stiffness slightly more forward compared to the first study.

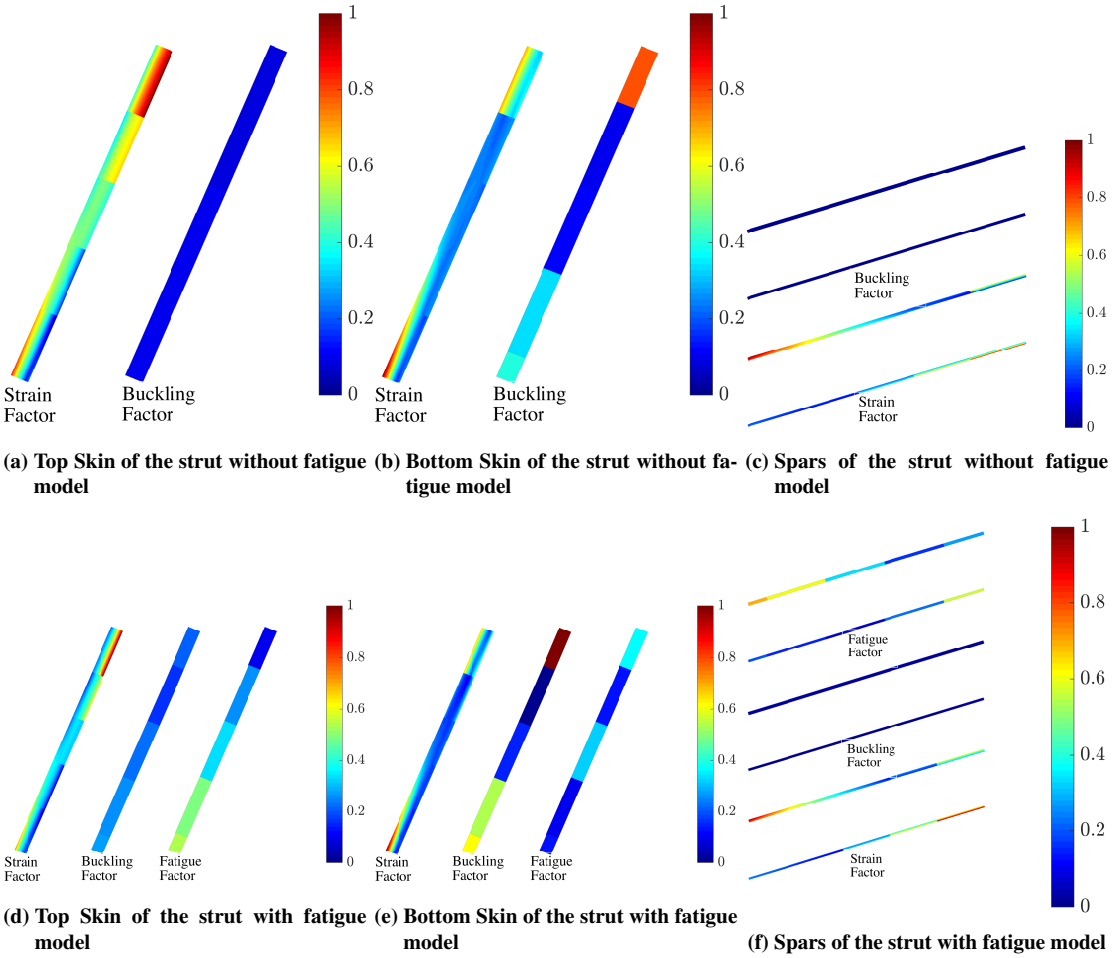

(a) Top Skin of the strut without fatigue model **(b) Bottom Skin of the strut without fatigue model** **(c) Spars of the strut without fatigue model**

(d) Top Skin of the strut with fatigue model **(e) Bottom Skin of the strut with fatigue model** **(f) Spars of the strut with fatigue model**

Figure 7: Value of the critical constraints for the strut of the optimized SBW.

Figure 11 compares the critical static and dynamic loads acting on the top and bottom skin of the wing of the optimized SBW for both the studies. For each laminate, the number indicates the critical flight point, and the colour indicates the critical gust gradient. The laminates with grey colour are critical with respect to the static load cases. Flight points 1, 2, 3 and 4 are static load cases described in Table 4 and the rest are the dynamic flight points as shown in Figure 6.

Looking at the thickness distribution, as expected, the optimized SBW in the first study where a knockdown of 68% is applied to the material allowables is thicker compared to the SBW in the second study. The weight of the SBW in the first study is 2,670 kg, whereas, in the second study, the SBW weighs at 2,100 kg. Thus, by including analytical fatigue model, the weight of

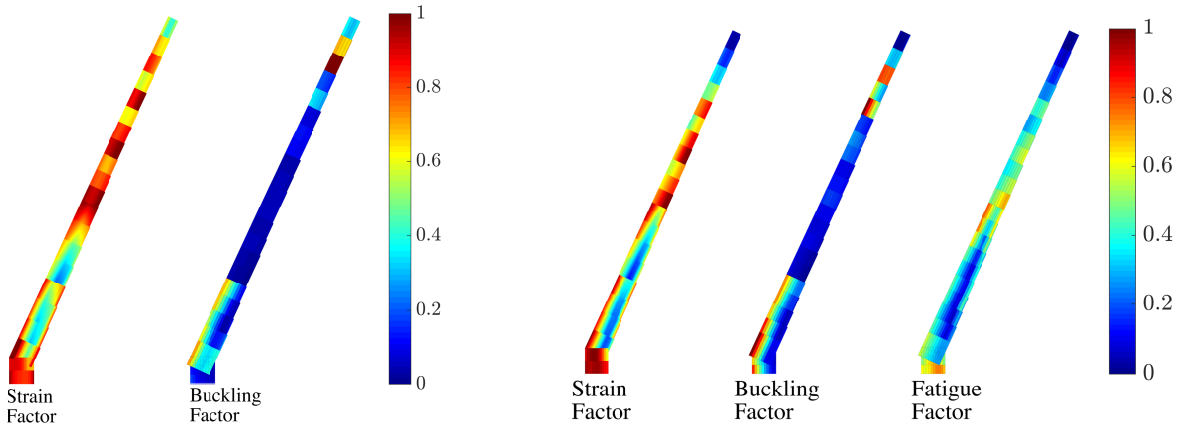

(a) Top Skin of the wing without fatigue model

(b) Top Skin of the wing with fatigue model

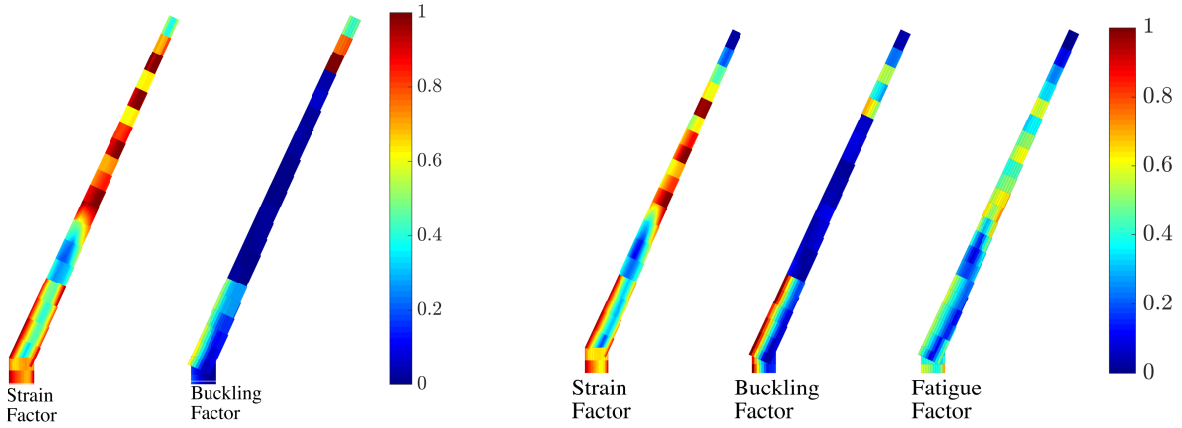

(c) Bottom Skin of the wing without fatigue model

(d) Bottom Skin of the wing with fatigue model

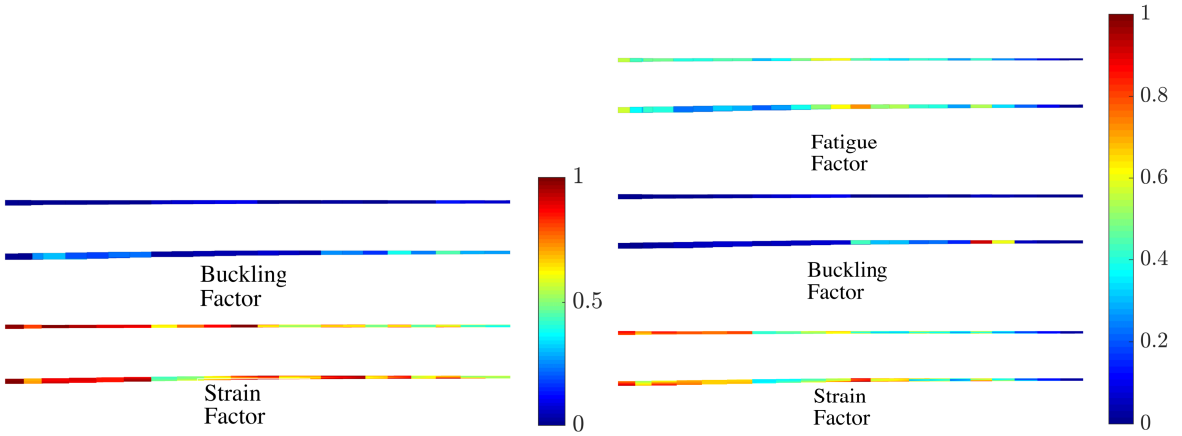

(e) Spars of the wing without fatigue model

(f) Spars of the wing with fatigue model

Figure 8: Value of the critical constraints for the wing of the optimized SBW.

the SBW can be reduced by approximately 22%.

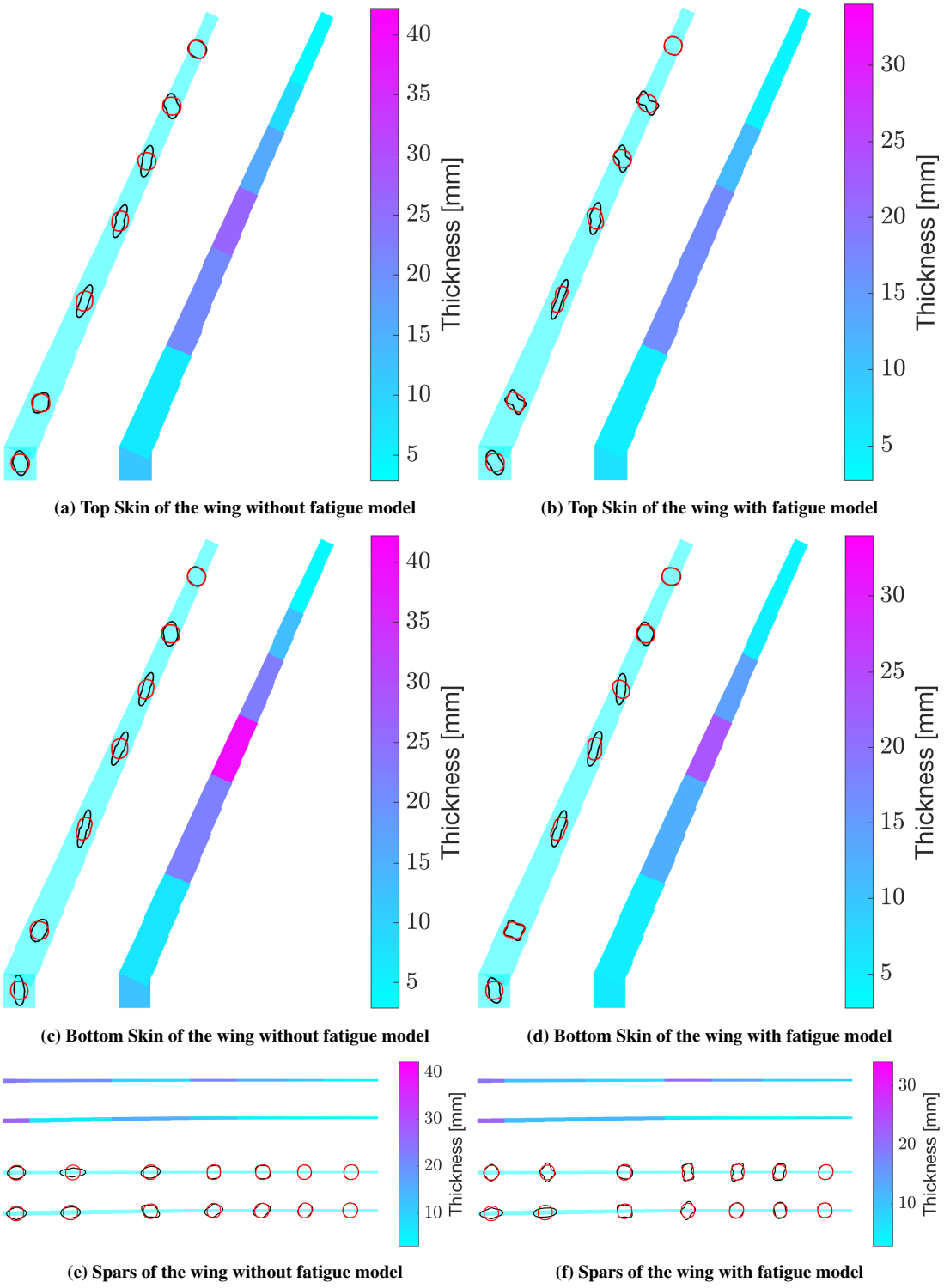

(a) Top Skin of the wing without fatigue model

(b) Top Skin of the wing with fatigue model

(c) Bottom Skin of the wing without fatigue model

(d) Bottom Skin of the wing with fatigue model

(e) Spars of the wing without fatigue model

(f) Spars of the wing with fatigue model

Figure 9: Stiffness and thickness distribution for the main wing of the optimized SBW (In-plane stiffness: black, out-of-plane stiffness: red).

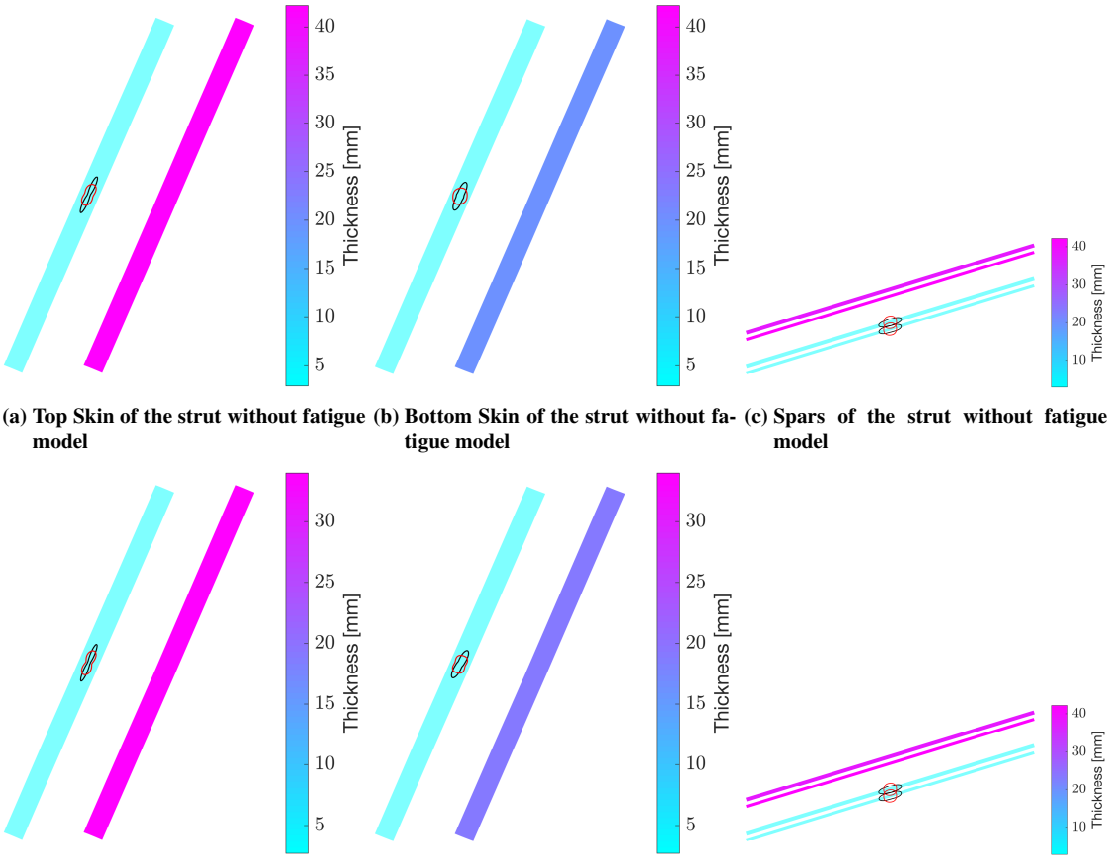

(a) Top Skin of the strut without fatigue model (b) Bottom Skin of the strut without fatigue model (c) Spars of the strut without fatigue model

(d) Top Skin of the strut with fatigue model (e) Bottom Skin of the strut with fatigue model (f) Spars of the strut without fatigue model

Figure 10: Stiffness and thickness distribution for the strut of the optimized SBW (In-plane stiffness: black, out-of-plane stiffness: red).

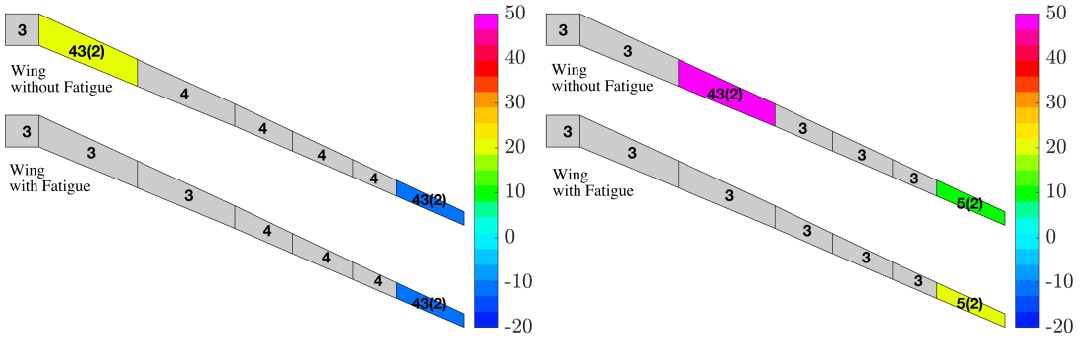

(a) Top Skin (b) Bottom Skin

Figure 11: Critical static and dynamic loads on the top and bottom skin of the optimized SBW

4. CONCLUSIONS

In this paper, a thickness and stiffness optimization of a composite SBW was performed. Previously developed methodologies were used to include critical gust loads and analytical fatigue model in the optimization process. The results show that a composite SBW is sized by both static as well as dynamic loads and hence they need to be taken into account with a dynamic aeroelastic solution instead of a quasi-steady solution.

Two optimization studies were conducted, one without the fatigue model and one with the fatigue model. In the latter study, the results show that the fatigue influences the optimized design by orienting the in plane stiffness a bit more forward compared to the first study. In the first study, to account for fatigue, a knockdown factor of 68% was applied to the strength allowables. As a result, the weight of the SBW in the case of the first study compared to the second study is higher by 22%.

5. REFERENCES

[1] Krein, A. and Williams, G. (2012). Flightpath 2050: Europe's vision for aeronautics. *Innovation for Sustainable Aviation in a Global Environment: Proceedings of the Sixth European Aeronautics Days, Madrid, 30 March-1 April, 2011*, 63.

[2] Smith, S. C. (1996). A computational and experimental study of nonlinear aspects of induced drag.

[3] Cavallaro, R. and Demasi, L. (2016). Challenges, ideas, and innovations of joined-wing configurations: a concept from the past, an opportunity for the future. *Progress in Aerospace Sciences*, 87, 1–93.

[4] Gur, O., Schetz, J. A., and Mason, W. H. (2011). Aerodynamic considerations in the design of truss-braced-wing aircraft. *Journal of Aircraft*, 48(3), 919–939.

[5] Gur, O., Bhatia, M., Schetz, J. A., et al. (2010). Design optimization of a truss-braced-wing transonic transport aircraft. *Journal of aircraft*, 47(6), 1907–1917.

[6] Mallik, W., Kapania, R. K., and Schetz, J. A. (2015). Effect of flutter on the multidisciplinary design optimization of truss-braced-wing aircraft. *Journal of Aircraft*, 52(6), 1858–1872.

[7] Meadows, N. A., Schetz, J. A., Kapania, R. K., et al. (2012). Multidisciplinary design optimization of medium-range transonic truss-braced wing transport aircraft. *Journal of Aircraft*, 49(6), 1844–1856.

[8] Bhatia, M., Kapania, R. K., and Haftka, R. T. (2012). Structural and aeroelastic characteristics of truss-braced wings: A parametric study. *Journal of Aircraft*, 49(1), 302–310.

[9] Gern, F. H., Naghshineh-Pour, A. H., Sulaeman, E., et al. (2001). Structural wing sizing for multidisciplinary design optimization of a strut-braced wing. *Journal of aircraft*, 38(1), 154–163.

[10] Bradley, M. K., Droney, C. K., and Allen, T. J. (2015). Subsonic ultra green aircraft research. phase ii-volume i; truss braced wing design exploration.

[11] Chakraborty, I., Nam, T., Gross, J. R., et al. (2015). Comparative assessment of strut-braced and truss-braced wing configurations using multidisciplinary design optimization. *Journal of Aircraft*, 52(6), 2009–2020.

[12] Khodaparast, H. H., Georgiou, G., Cooper, J. E., et al. (2012). Efficient worst case 1-cosine gust loads prediction. *Journal of Aeroelasticity and Structural Dynamics*, 2(3).

[13] Rajpal, D., Gillebaart, E., and Breuker, R. D. (2019). Preliminary aeroelastic design of composite wings subjected to critical gust loads. *Aerospace Science and Technology*, 85, 96 – 112. ISSN 1270-9638. doi:https://doi.org/10.1016/j.ast.2018.11.051.

[14] Rajpal, D., Kassapoglou, C., and De Breuker, R. (2018). Aeroelastic optimization of composite wings subjected to fatigue loads. In *2018 AIAA/ASCE/AHS/ASC Structures, Structural Dynamics, and Materials Conference*. p. 0227.

[15] Werter, N. P. M. and De Breuker, R. (2016). A novel dynamic aeroelastic framework for aeroelastic tailoring and structural optimisation. *Composite Structures*, 158, 369–386. ISSN 0263-8223. doi:10.1016/j.compstruct.2016.09.044.

[16] Werter, N. P. M., De Breuker, R., and Abdalla, M. M. (2017). Continuous-time state-space unsteady aerodynamic modeling for efficient loads analysis. *AIAA Journal*, 1–12.

[17] Svanberg, K. (2002). A class of globally convergent optimization methods based on conservative convex separable approximations. *SIAM journal on optimization*, 12(2), 555–573.

[18] Kassapoglou, C. (2007). Fatigue life prediction of composite structures under constant amplitude loading. *Journal of Composite Materials*, 41(22), 2737–2754.

[19] Kassapoglou, C. (2010). Fatigue of composite materials under spectrum loading. *Composites Part A: Applied Science and Manufacturing*, 41(5), 663–669.

[20] Kassapoglou, C. (2011). Fatigue model for composites based on the cycle-by-cycle probability of failure: implications and applications. *Journal of Composite Materials*, 45(3), 261–277.

[21] Tsai, S. and Pagano, N. (1968). Invariant Properties of Composite Materials. In *Composite Materials Workshop*. Westport: Technomic Publishing Co., pp. 233–253.

[22] Khani, A., IJsselmuiden, S. T., Abdalla, M. M., et al. (2011). Design of variable stiffness panels for maximum strength using lamination parameters. *Composites Part B: Engineering*, 42(3), 546–552.

[23] Lowak, H., DeJonge, J., Franz, J., et al. (1979). Minitwist - a shortened version of twist. *NLR MP 79018 U*.

[24] Torrigiani, F., Bussemaker, J., Ciampa, P., et al. (2018). Design of the strut braced wing aircraft in the agile collaborative mdo framework. In *International Council of the Aeronautical Science*.

[25] Rajpal, D., De Breuker, R., Torrigiani, F., et al. (2018). Including aeroelastic tailoring in the conceptual design process of a composite strut braced wing. In *International Council of the Aeronautical Science*.

[26] Ciampa, P. D. and Nagel, B. (2017). The agile paradigm: the next generation of collaborative mdo. In *18th AIAA/ISSMO multidisciplinary analysis and optimization conference*. p. 4137.

[27] Hammer, V. B., Bendsøe, M., Lipton, R., et al. (1997). Parametrization in laminate design for optimal compliance. *International Journal of Solids and Structures*, 34(4), 415–434.

[28] Raju, G., Wu, Z., and Weaver, P. (2014). On further developments of feasible region of lamination parameters for symmetric composite laminates. In *55th AIAA/ASMe/ASCE/AHS/SC Structures, Structural Dynamics, and Materials Conference*. p. 1374.

[29] Wu, Z., Raju, G., and Weaver, P. M. (2015). Framework for the buckling optimization of variable-angle tow composite plates. *AIAA Journal*, 53(12), 3788–3804.

[30] Dillinger, J., Klimmek, T., Abdalla, M. M., et al. (2013). Stiffness optimization of composite wings with aeroelastic constraints. *Journal of Aircraft*, 50(4), 1159–1168.

COPYRIGHT STATEMENT